Charge-transfer complexes of conjugated polymers as intermediates in charge photogeneration for organic photovoltaics

Bakulin, Artem A.; Martyanov, Dmitry; Paraschuk, Dmitry Yu.; van Loosdrecht, Paul H. M.; Pshenichnikov, Maxim S.

Published in:
Chemical Physics Letters

DOI:
10.1016/j.cplett.2009.09.052

Publication date:
2009

Chemical Physics Letters 482 (2009) 99–104

Contents lists available at ScienceDirect

Chemical Physics Letters

journal homepage: www.elsevier.com/locate/cplett

Charge-transfer complexes of conjugated polymers as intermediates in charge photogeneration for organic photovoltaics

Artem A. Bakulin [a,*], Dmitry Martyanov [b,c], Dmitry Yu. Paraschuk [b,c], Paul H.M. van Loosdrecht [a], Maxim S. Pshenichnikov [a]

[a] Zernike Institute for Advanced Materials, University of Groningen, Nijenborgh 4, 9747 AG Groningen, The Netherlands
[b] Faculty of Physics, Lomonosov Moscow State University, Leninskie Gory, 119991 Moscow, Russia
[c] Lebedev Physical Institute, RAS, Leninsky ave. 53, 119991 Moscow, Russia

ARTICLE INFO

Article history:
Received 16 July 2009
In final form 15 September 2009
Available online 18 September 2009

ABSTRACT

Ultrafast visible-pump/IR-probe spectroscopy is applied to study the wavelength dependence of charge photogeneration in materials based on donor–acceptor charge-transfer complexes (CTCs) of the conjugated polymer MEH-PPV. In binary polymer–acceptor blends, photoexcitation in the absorption band of either CTC or polymer results in similar dynamics of the charge-associated transient absorption. Likewise, in polymer/CTC–acceptor/fullerene ternary blends, where charge separation occurs via a two-step pathway, the photophysics is also independent of excitation wavelength. These similarities in charge dynamics indicate that CTC excited states serve as an intermediate for charge photogeneration. The conclusions of the ultrafast study are supported by photocurrent spectroscopy.

1. Introduction

The improvement in the efficiency of plastic solar cells requires advanced management of the electronic structures of the materials in order to balance the optical gap, open circuit voltage, and charge separation/transport efficiency in the cell. The energy levels of the highest occupied molecular orbital (HOMO) and the lowest unoccupied molecular orbital (LUMO) of the donor and acceptor are among the main parameters for such optimization. This promoted synthesis of a great variety of different polymers and fullerene derivatives. However, controlling and adjusting the properties of pristine donor and acceptor materials does not directly affect the charge dynamics in their blend. For instance, recent studies [1–6] have indicated that charge photogeneration in polymer–fullerene blends occurs mostly via an intermediate state(s) at the polymer–fullerene interface [7,8]. These states are associated with the weak charge-transfer complex (CTC) which is formed between polymer donor and fullerene acceptor. Because the donor–acceptor blends in efficient organic solar cells are phase-separated, there are three manifolds of electronic states associated with the donor (polymer), acceptor (fullerene), and their CTC, respectively. As a result, formation of free charges in the blends takes place in at least two steps, where the second step includes charge transfer from the CTC to the acceptor and/or donor materials. Obviously, the efficiency of such a charge-transfer process depends on many factors including, apart from properties of pristine donor and acceptor, the energy of CTC states [3], the excess energy provided by absorbed photon [9], and local blend morphology.

A direct study of charge generation through the CTC states in the polymer–fullerene blends is possible [10] but quite challenging because, first, the CTC absorption band is not very pronounced, and, second, it partly overlaps with the fullerene absorption. Therefore, it would be advantageous to start with a material where all three manifolds of states (donor, acceptor, and CTC) are easily distinguishable. In our previous work [11], we suggested that ternary blends of a conjugated polymer with low-molecular-weight acceptors [12] and fullerene can serve as the model for such a kind of system. In the ternary blend, the initial charge separation occurs within the donor–acceptor pair that forms a pronounced CTC. After that, the electron is further transferred to the fullerene and then diffuses away from the hole [11].

In previous studies [11,13], the main emphasis was put on the ultrafast charge recombination and the very possibility of the consecutive charge transfer for which the excitation wavelength was deliberately chosen to coincide with CTC absorption band. However, there remains one important but still unaddressed question that concerns the general prevalence of the CTC-mediated charge separation: Does the direct photoexcitation of the polymer provide charge generation via the same CTC states as the excitation of the charge-transfer band? The answer has far-reaching consequences for fundamental understanding of the photophysics in the donor–acceptor blends as well as for the development of CTC-based photovoltaic materials.

In this Letter, the early-time dynamics of photoinduced charges in materials with CTCs formed between MEH-PPV and organic

* Corresponding author. Fax: +31 50 3634441.
E-mail address: A.A.Bakulin@rug.nl (A.A. Bakulin).

0009-2614/$ - see front matter © 2009 Elsevier B.V. All rights reserved.
doi:10.1016/j.cplett.2009.09.052

acceptors are investigated using time-resolved photoinduced absorption (PIA) spectroscopy. We observed that *regardless* the particular excitation wavelength (be it in the charge-transfer band or in the polymer absorption band) the photoexcitation of the binary CTC blends results in sub-100 fs generation of localized charges being followed by fast and pronounced geminate recombination. Excitation energy invariance also extends to the ternary blends of CTC and fullerenes (C_{60}), where the recombination is suppressed by formation of a new charge-transfer pathway from CTC to C_{60}. The similarities in charge dynamics indicate that the CTC excited states serve as an efficient intermediate for the charge photogeneration in all the materials studied. The conclusions of the ultrafast experiments are confirmed by studying the long-time behavior of charges in CTC-based materials with a photocurrent spectroscopy.

2. Experimental

The photoinduced absorption (PIA) spectroscopy is built upon the fact that surplus charge on a conjugated molecule induces new allowed states inside its optical gap, thereby forming additional absorption bands in the IR spectral range. The well-known fingerprints of charged states in the widely-studied conjugated polymer MEH-PPV are the low energy (LE) and high energy (HE) absorption bands at ~0.5 and 1.3 eV, respectively [14]. An ultrafast modification of PIA utilizes a pair of pulses one of which excites charges in the polymer while another probes the time-dependent concentration of the photogenerated charges by monitoring the IR charge-induced bands. An additional option, which potential is still to be exploited in organic photovoltaics, is the polarization-sensitive version of PIA, where the change of the polarization state of the HE [15–17] and LE probe [13] is observed, thereby providing information on charge and energy transfer in the polymer.

Time- and spectrally-resolved PIA experiments were performed using setup described in Ref. [13]. A home-built Ti:Sapphire amplifier was used to pump a noncollinear optical parametric amplifier providing visible excitation pulses (40 fs, 10 nJ per pulse) and an optical parametric amplifier providing the IR probe [18]. The 5 nJ probe pulses, with duration of ~70 fs and a bandwidth of ~300 cm^{-1} FWHM, were positioned in the center of the LE polaron band at 3300 cm^{-1}. The polarization of the IR-probe beam was rotated by 45° with respect to the polarization of the visible pump beam. After the sample, the probe component parallel or perpendicular to the pump was selected by a wire-grid polarizer (extinction 1:100) and detected by a InSb photodiode. All time-resolved PIA data were obtained at 300 K under nitrogen flow.

A variety of blends of the following materials were used (Fig. 1): poly[2-methoxy-5-(2′-ethyl-hexyloxy)-1,4-phenylene vinylene] (MEH-PPV), 1,5-dinitroantraquinone (DNAQ), 2,4,7-trinitrofluorenone (TNF) and fullerene C_{60}. We chose the C_{60} fullerene instead of its widely-used soluble derivative PCBM because of its ~0.1 eV higher electron affinity as compared to PCBM. The higher electron affinity warrants the increase of the driving force in the DNAQ/fullerene and/or TNF/fullerene electron transfer. Indeed, our preliminary experiments on MEH-PPV/DNAQ/PCBM blends indicated a modest increase in the charge generation efficiency only, in sharp contrast with the results of Ref. [11] where the C_{60} addition resulted in a substantial enhancement of the long-lived charge production.

During the preparation of binary and ternary blends each component was separately dissolved in chlorobenzene at a concentration of 2 g/l. Films were drop-casted on microscope cover-glass substrates and typically had a ~200 nm thickness. The donor–acceptor ratios in MEH-PPV/DNAQ and MEH-PPV/TNF blends were chosen 1:0.3 to provide the maximum CTC concentration in the films [19]. For preparation of ternary blends the solutions were mixed with weight ratios of the components MEH-PPV/CTC-acceptor/C_{60} of 1/0.3/0.2. The absorption spectra were recorded with a Perkin Elmer Lambda 900 spectrophotometer.

For the photocurrent measurements, sandwich-type samples were prepared on ITO-covered glass substrates. A PEDOT:PSS layer was spin-cast onto the ITO-side. Next, an active layer of MEH-PPV/acceptor chlorobenzene solution was spin-cast (at 1000 rpm) on top of the PEDOT:PSS layer. The active layer absorbed less than 50% of the incident light (the thickness did not exceed 50 nm) so that internal filter effects can be ruled out. The small sample thickness also allowed us to disregard interference and sample-thickness effects [20,21] which could potentially influence the measured external quantum efficiency (EQE) [22]. For instance, the modulation of EQE spectra in the 500–650 nm region is estimated to be no more than 10% with 20% variations in the sample thickness. Aluminum contacts were thermally deposited onto the active layer. The active layers of the photodiodes were illuminated through the substrate by a tungsten-halogen lamp, and the photocurrent was, after preamplification, measured by a lock-in amplifier at a 75 Hz modulation frequency.

3. Results and discussion

Fig. 2 compares the optical absorption spectra of the donor polymer MEH-PPV, binary donor–acceptor blends (MEH-PPV/C_{60}, MEH-PPV/DNAQ, MEH-PPV:TNF), and ternary MEH-PPV/DNAQ/C_{60} blend. The extinction coefficient of TNF and DNAQ is negligible in the depicted spectral range. Within the experimental accuracy, the absorption spectrum of the MEH-PPV/C_{60} blend is a superposition of the individual spectra of MEH-PPV and C_{60} indicating a relatively weak CTC oscillator strength in the MEH-PPV/C_{60} blend [7]. On the other hand, MEH-PPV/DNAQ and MEH-PPV/TNF blends display a red shift of the MEH-PPV main absorption band and an

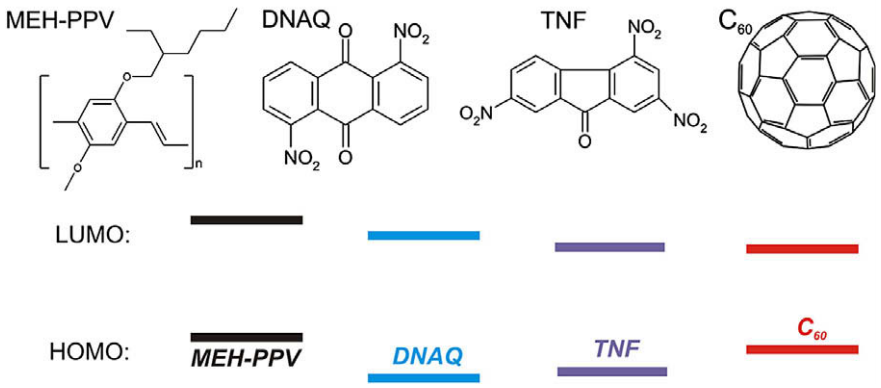

Fig. 1. The chemical structure of materials under study and their energy diagram of the frontier molecular orbitals.

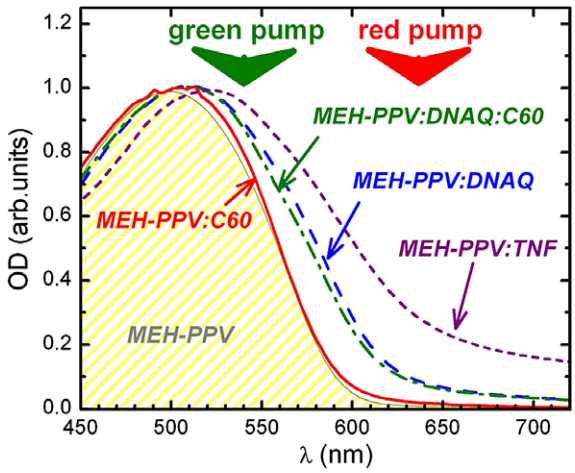

Fig. 2. Normalized absorption spectra of (1:0.2) MEH-PPV/C_{60}, (1:0.3) MEH-PPV/DNAQ, (1:0.3) MEH-PPV/TNF and (1:0.3:0.2) MEH-PPV/DNAQ/C_{60} blends. The shaded contour represents the absorption of a neat MEH-PPV film. The green and red arrows show the central wavelengths for polymer and CTC band excitations. (For interpretation of the references to color in this figure legend, the reader is referred to the web version of this article.)

additional absorption shoulder extending into the optical gap of MEH-PPV. These changes are associated with the formation of pronounced CTC in the blends [12,19]. Photoluminescence of MEH-PPV in the ternary blends (not shown here) is quenched by three orders of magnitude which is ~10 times more efficient than the photoluminescence quenching observed in MEH-PPV/C_{60}. This provides the first indication that exciton dissociation in the ternary blend occurs mostly due to charge separation at the CTC formed between MEH-PPV and either DNAQ or TNF acceptor [12].

Remarkably, the CTC absorption in polymer–acceptor blends is not related to the acceptor electron affinity. In fact, in blends with MEH-PPV, the weaker DNAQ acceptor results in more intense CTC absorption as compared to the stronger fullerene acceptor. Moreover, earlier studies did not find any signatures of CTC in blends of conjugated polymers with such a strong electronic acceptor as TCNQ and its derivatives [23]. Following the Mulliken's model [24], we have suggested that the overlap of the corresponding frontier molecular orbitals (donor's HOMO and acceptor's LUMO) is an important factor for CTC formation [11,25]. Therefore, elongated acceptors with a better match to the extended molecular orbitals of the conjugated chain are more beneficial for higher CTC absorption. This also explains the very weak polymer–fullerene CTC given the poor overlap between the spheroidal fullerene LUMO and the ribbon-type polymer HOMO. In contrast, the much more intensive CTC absorption in the blends with DNAQ and TNF can be assigned to better overlap between the corresponding molecular orbitals.

Top panels in Fig. 3 compare isotropic PIA transients in different binary blends after excitation at 650 nm where MEH-PPV is almost transparent (open symbols), and near the maximum of the polymer absorption band at 540 nm (solid symbols). In either MEH-PPV/DNAQ or MEH-PPV/TNF CTC, the red (650 nm) optical pumping corresponds to direct photoexcitation of the charge-transfer band. The complementary measurements on the binary MEH-PPV/DNAQ and MEH-PPV/TNF CTCs with excitation at 620 and 800 nm (not discussed in the current Letter) did not display any essential difference of the PIA transients as compared to those observed at 650 nm. The PIA traces for the CTCs are dominated by a prominent and fast multi-exponential decay previously explained by geminate recombination of photogenerated charges [13]. The PIA transients obtained at 540 nm are similar to those observed after excitation into the CTC band. The similarity of PIA kinetics at the red and green excitation indicates that charge photogeneration occurs through the same CTC states in the both cases. As follows from Fig. 3a and b, for the MEH-PPV/DNAQ and MEH-PPV/TNF CTCs the amount of long-lived charges excited at 540 nm is somewhat higher than that at 650 nm. This signifies that the 'hot' CTC excitons have a slightly higher probability to dissociate into long-lived charges. Note that at the acceptor concentration used, almost all the polymer conjugated segments are involved in the CTC [19]; therefore, the contribution to the PIA from polymer segments not involved in CTCs, is insignificant.

The measured isotropic transients match well the observations recently reported by Holt et al. (20%, or 1:0.25 ratio of acceptor in the legend in Fig. 7 of Ref. [26]) for excitation above and below the polymer optical gap in the MEH-PPV/TNF blend (note that this paper misquotes TNF concentration used in Ref. [13]: allegedly 1% instead of the correct value of 25%). In contrast, the transients reported for the blend ratio 1:1 are different from those for 1:0.25 [26] and from those reported in this work. For instance, the long-lived component changes its behavior from more pronounced for below-gap excitation to much less pronounced for above-gap excitation [26]. Such behavior falls off from the general trend observed for acceptor concentrations below the 1:0.3 ratio. The difference most probably originates from a substantial change in the blend morphology at concentrations higher than 1:0.3. Indeed, previous Raman [19] and Rayleigh [27] light-scattering studies demonstrated that if the TNF content exceeds 30%, CTC concentration reaches a saturation level, and excess TNF forms phase-separated domains which can affect recombination of charges. In this respect, a 1:0.3 concentration is optimal as almost all acceptors are involved in the CTCs and there is still no phase separation in the blend.

In contrast to the blends with a pronounced CTC formation, the PIA transient for the MEH-PPV/C_{60} blend (where CTC transition oscillator strength is relatively weak) [7] displays a minor decay, thereby indicating that the majority of induced charges are long-lived (Fig. 3c). Thus, isotropic transients for different blends show an interesting trend: the efficiency of charge recombination increases with the increasing oscillator strength of the CTC transition (Fig. 2). Such behavior can be explained in the frame of Mulliken's model [24]. The efficiency of recombination is proportional to the overlap between the wave functions of ground and charge-separated states. This overlap is, in turn, related to the shift of electron density from donor to acceptor in the ground state, and, therefore, to the value of CTC-transition dipole moment.

Lower panels in Fig. 3 compare evolution of the PIA anisotropy in the binary blends following red and green excitation. In the MEH-PPV/C_{60} blend the anisotropy immediately after excitation is low (Fig. 3f) and keeps on decaying with time as a result of energy and charge transport [13]. In contrast, the transient anisotropies in both the MEH-PPV/TNF and MEH-PPV/DNAQ blends have high initial values and stay persistently at high levels for both excitation wavelengths. The anisotropy behavior after the excitation into the CTC band was previously assigned [13] to localization of charges within the parent CTC chain and/or with high local order of conjugated segments involved in the CTC. The main feature that the anisotropy stays constant within the ~10 ps recombination time, was also confirmed by recent studies of Holt et al. [26]. The anisotropy increase at longer times was previously explained as interplay between responses of the short- and long-lived subensembles due to the fact that anisotropy is not an additive value [13]. The different long-time dynamics of anisotropy reported by Holt et al. [26] could be a consequence of a variety of factors, like different pump and probe wavelengths, excitation repetition rate, and sample morphology.

The similarities in the anisotropy dynamics observed at different excitation wavelengths, support our conclusion about the

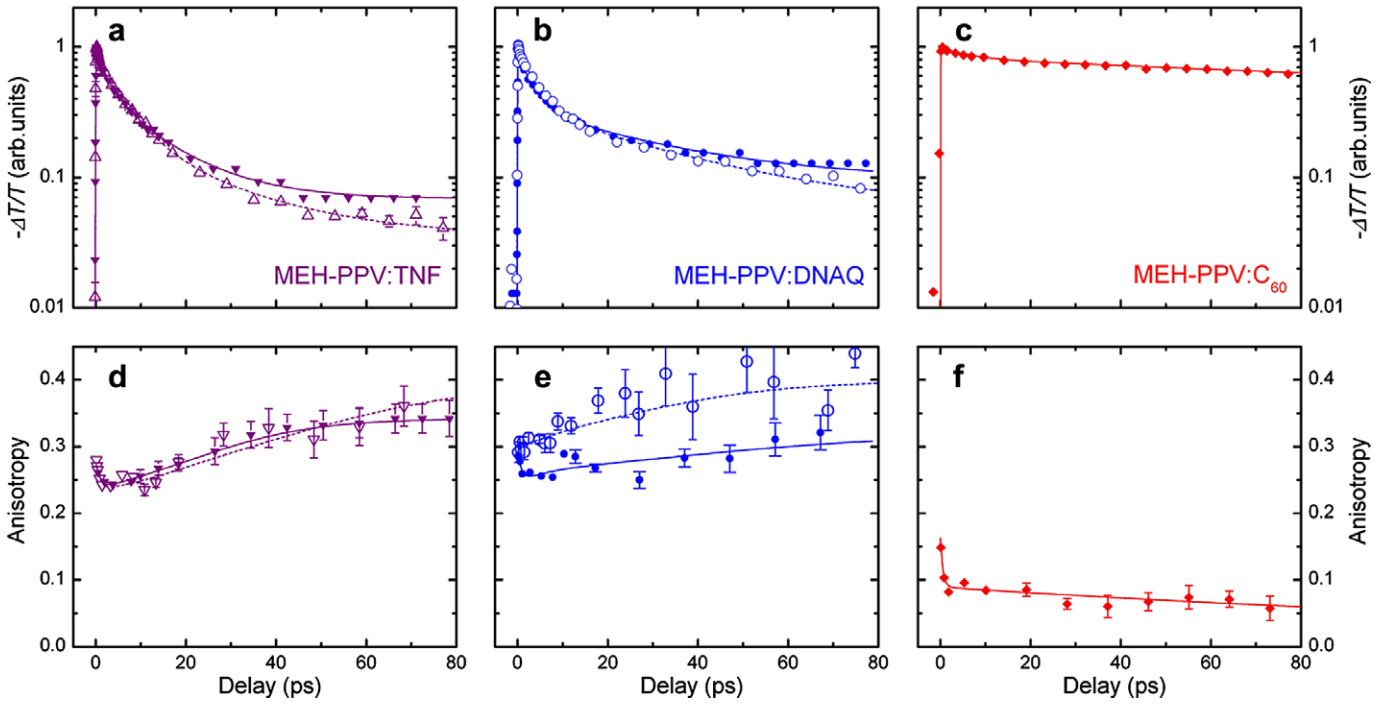

Fig. 3. Isotropic PIA (top) and transient anisotropy (bottom) of the LE band in MEH-PPV/TNF (a, d), MEH-PPV/DNAQ (b, e), and CTCs and MEH-PPV/C_{60} (c, f) blend excited at 650 nm (open symbols) and 540 nm (solid symbols). Solid curves represent multi-exponential fits to the data meant to guide the eye. Isotropic data are normalized to their maximum values. For MEH-PPV/C_{60} the transients for 650 nm excitation are not shown because of their low amplitude due to small absorption in that region.

involvement of the charge-transfer state in the light-to-charge conversion at very different photon energies. Particularly, the high initial anisotropy value implies that generation of charges is not preceded by the intermediate intramolecular exciton states typical for conjugated polymers [28]. At longer delay times, the anisotropy level with green excitation (i.e. into the polymer absorption band) is only slightly lower than that with red excitation (direct CTC absorption). Similarly to the isotropic PIA, this is indicative of a minor effect of the ~0.4 eV excess energy on the long-term charge separation efficiency.

Fig. 4 presents isotropic transients at the wavelength of the LE PIA band in the ternary blends of MEH-PPV/DNAQ/C_{60} (a, c) and MEH-PPV/TNF/C_{60} (b, d), at red (620 nm) and green (540 nm) excitation; the data for the binary blends are also shown for direct comparison. The PIA decays in the ternary MEH-PPV/TNF/C_{60} blend at either frequency are almost undistinguishable from those in the MEH-PPV/TNF CTC. This signifies that the excess energy provided by the 540 nm excitation does not lead to creation of additional long-lived charges in the ternary blend as compared to its binary counterpart. Hence, in the MEH-PPV/TNF/C_{60} blend the excitation reaches the CTC state and becomes localized within the donor–acceptor pair independently of the initial absorption into the polymer or charge-transfer band. Further charge separation appears to be unlikely due too the small difference in LUMO energies between TNF and C_{60} [11].

In sharp contrast to the TNF case, the PIA transients in the ternary blend MEH-PPV/DNAQ/C_{60} (Fig. 4b and d) are significantly different from those in the binary MEH-PPV/DNAQ blend. As we have demonstrated before [11] the ternary MEH-PPV/DNAQ/C_{60} blend provides a more efficient generation of long-lived charges as compared to MEH-PPV/DNAQ when excited into the CTC band (Fig. 4b). This was attributed to a consecutive electron transfer from the DNAQ to the fullerene within the first few ps after excitation, aided by the difference in LUMO levels. Surprisingly, PIA transients in the MEH-PPV/DNAQ/C_{60} ternary blend excited in the polymer absorption (Fig. 4d) do not differ much from those with the CTC excitation. This evidences that the charge generation and transfer follow the same pathway in both cases which is only possible if the charge separation in the ternary blend occurs similarly to the binary one, i.e. solely via the CTC states. Furthermore, for 540 nm excitation wavelength, the geminate recombination is more pronounced in the ternary blend than in MEH-PPV/C_{60} blend (Fig. 4d). This occurs because consecutive charge transfer is not 100% efficient; our previous estimate yielded ~30% efficiency after excitation into the CTC band [11]. The incompletely suppressed geminate recombination of CTC charge-separated states results in decreasing of the EQE (*vide infra*).

As follows from the time-resolved data, the photophysics in the ternary blends cannot be treated as a simple superposition of the independent processes in the corresponding binary blends. In the MEH-PPV/DNAQ/C_{60} blend, the nonadditive behavior originates from a consecutive character of the process: the electron is first transferred to DNAQ and only then to the fullerene [11]. In the MEH-PPV/TNF/C_{60}, the presence of TNF completely excludes C_{60} from the photophysics in the blend. This can be a consequence of several factors. First, for MEH-PPV/TNF ratio used (1:0.3), almost each conjugated segment of polymer is involved in the CTC [19] and, therefore, the CTC state is readily available. Second, due to strong absorption in the optical gap of MEH-PPV, the CTC can work as an efficient energy trap, collecting all the excitons formed at MEH-PPV via resonant energy transfer to the CTC [29] before they have dissociated into charges at the MEH-PPV/C_{60} interface.

Fig. 5a shows photocurrent action spectra of photodiodes with ternary blend, MEH-PPV/DNAQ CTC, and pure polymer used as the active layers. In agreement with the spectroscopic data (Fig. 4b and d), addition of C_{60} to the MEH-PPV/DNAQ blend increases the EQE of the photodiodes by more than one order of magnitude in visible and by almost three orders in the MEH-PPV optical gap. Absolute values of EQE in the MEH-PPV/C_{60} and ternary MEH-PPV/DNAQ/C_{60} blends are comparable (Fig. 5b). As

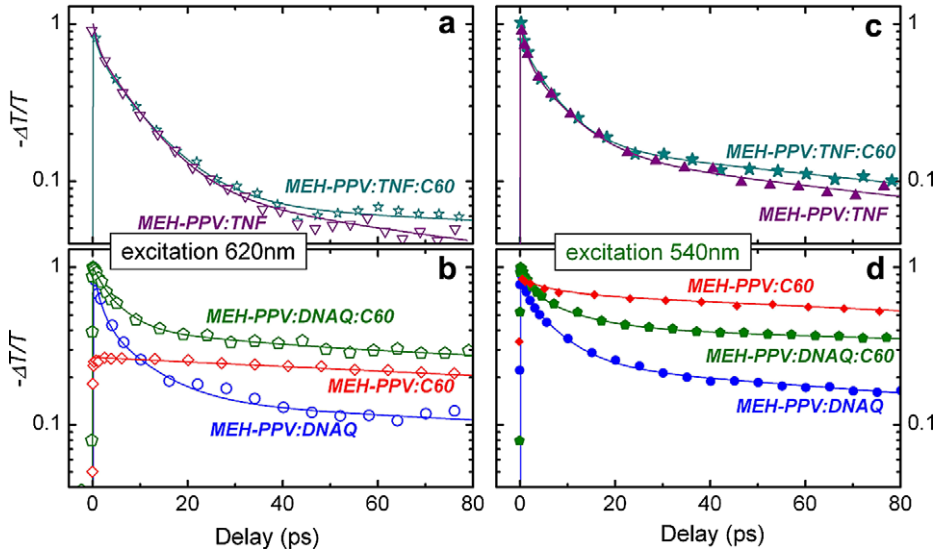

Fig. 4. Transient PIA of the LE band in binary and ternary blends after excitation at 620 nm (a, b) and 540 nm (c, d). Upper plots compare PIA in MEH-PPV/TNF (triangles) and MEH-PPV/TNF/C_{60} (stars) blends. Bottom plots compare MEH-PPV/DNAQ (circles), and MEH-PPV/C_{60} (diamonds) blends to the ternary MEH-PPV/DNAQ/C_{60} blend (pentagons). The PIA transients in each panel are normalized according to the maximum of absorption bands to account for variations in samples thickness, but not scaled otherwise. Solid lines represent multi-exponential fits to the data to guide the eye.

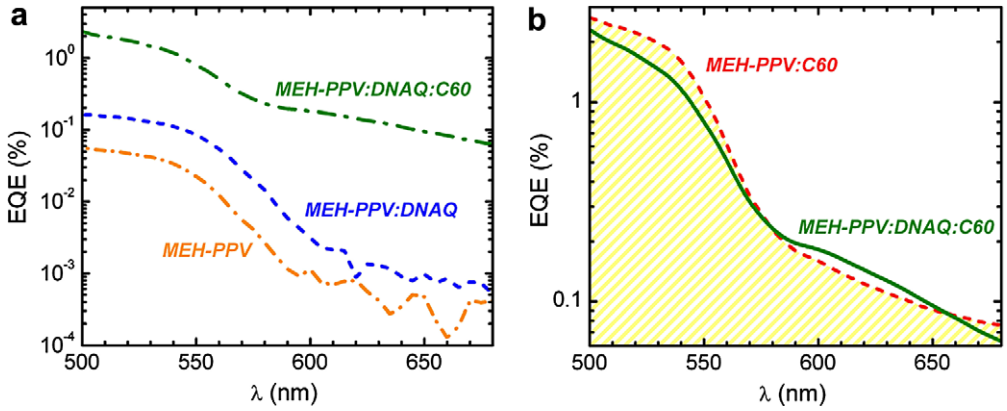

Fig. 5. (a) Photocurrent action spectra of photodiodes containing MEH-PPV (orange short-dash-dotted curve), MEH-PPV/DNAQ (blue dashed curve) and MEH-PPV/DNAQ/C_{60} (green dash-dotted curve) films as an active layer. (b) Direct comparison of photocurrent action spectra of the MEH-PPV/C_{60} (red dashed curve and shaded contour) and MEH-PPV/DNAQ/C_{60} (green solid curve) based photodiodes. (For interpretation of the references to color in this figure legend, the reader is referred to the web version of this article.)

expected [11], the EQE in the ternary blend noticeably increases (up to 30%) in the red flank of the spectrum as compared to MEH-PPV/C_{60} due to the formation of MEH-PPV/DNAQ CTC which extends the photosensitivity of the material into the red. In the green part of the spectrum the EQE of the ternary blend device is lower, which is in also line with the results of ultrafast measurements (Fig. 4d) of incompletely suppressed geminate recombination of CTC charge-separated states. Similarly, the increase of EQE in the red flank is clearly correlated with the change of the absorption spectra (Fig. 2) and with the isotropic PIA transients (Fig. 4b). Furthermore, the PIA data at the millisecond time scale also indicate higher red photosensitivity of the ternary blends as compared to its binary counterpart [11]. All these signify that the observed changes in EQE are not due to interference effects in the active layer of the device [20,21].

Finally, we would like to comment on the similarities between the photophysics in the ternary MEH-PPV/DNAQ/C_{60} blend and phase-separated binary MEH-PPV/C_{60} blends [1,3,4,6]. In both cases, CTCs between the polymer and the acceptor (C_{60} or DNAQ) are responsible for the initial transformation of an exciton into a geminate charge pair and, therefore, serve as an intermediate state in charge photogeneration. However, apart from the interfacial (CTC) manifold, an additional manifold(s) of electronic states is required to promote efficient separation of the geminate pair into a pair of long-lived charges, as provided, for instance, by pristine donor or/and pristine acceptor [30]. In the phase separated polymer-fullerene blends, CTCs are located at the polymer-fullerene interface, from which an efficient electron and hole injection occurs into the fullerene and polymer domains, respectively. In contrast, binary polymer–acceptor blends with a relatively strong ground-state charge-transfer interaction are homogeneous up to relatively high acceptor concentrations [27]. This explains the observations that the binary blends of MEH-PPV with fullerene display very different yield of long-lived charges compared to blends with TNF (or DNAQ) [13,26]. However, the yield of long-lived charges drastically increases when an additional manifold of electron-accepting states is introduced into the MEH-PPV:DNAQ blend by fullerene doping. From this perspective, it is interesting to note

that an increase of TNF content from 20% (homogeneous blend) to the 50% (TNF domain formation) [27] level, noticeably increases the lifetime of charges generated after red excitation [26].

4. Conclusion

We have performed a study of charge photogeneration in binary and ternary blends of a conjugated polymer MEH-PPV, with three organic acceptors: TNF, DNAQ, and C_{60}. According to the current understanding, all three acceptors form a ground-state charge-transfer complex (CTC) with MEH-PPV; but for TNF and DNAQ the CTCs are by far more pronounced than for C_{60}. We have observed that charge photogeneration dynamics in films with CTC formation do not depend on the energy of the absorbed photon. The CTC photoexcitation always results in sub-100 fs generation of charges followed by fast and pronounced geminate recombination, regardless whether the charge-transfer or donor absorption band is excited. Similarly, the charge dynamics are only weakly dependent on the pump photon energy in ternary blends of CTC and fullerene C_{60}. This signifies, that, independently of photon energy, charge separation always occurs in two steps; first an electron is transferred to the CTC acceptor and then to the acceptor that is much less involved in the ground-state interaction with the donor. Therefore, our experiments demonstrate that the low-energy excited states of the CTC are key intermediates for charge generation in the donor–acceptor blends with charge-transfer interaction.

Acknowledgements

We thank J. Krylova for photoluminescence measurements, A. Gromchenko and E. Nechvolodova for help in devices preparation, J.C. Hummelen and V.V. Krasnikov for many fruitful discussions. This study was in part financially supported by the Russian Foundation for Basic Research (project 08-02-12170-ofi).

References

[1] I.-W. Hwang et al., Adv. Mater. 19 (2007) 2307.
[2] D. Veldman et al., J. Am. Chem. Soc. 130 (2008) 7721.
[3] H. Ohkita et al., J. Am. Chem. Soc. 130 (2008) 3030.
[4] I.-W. Hwang, D. Moses, A.J. Heeger, J. Phys. Chem. C 112 (2008) 4350.
[5] M. Hallermann, S. Haneder, E.D. Como, Appl. Phys. Lett. 93 (2008) 053307.
[6] D. Veldman, S.C.J. Meskers, R.A.J. Janssen, Adv. Funct. Mater. 19 (2009) 1939.
[7] L. Goris et al., J. Mater. Sci. 40 (2005) 1413.
[8] J.J. Benson-Smith et al., Adv. Funct. Mater. 17 (2007) 451.
[9] V.I. Arkhipov, E.V. Emelianova, H. Bassler, Phys. Rev. Lett. 82 (1999) 1321.
[10] T. Drori, C.-X. Sheng, A. Ndobe, S. Singh, J. Holt, Z.V. Vardeny, Phys. Rev. Lett. 101 (2008) 037401.
[11] A.A. Bakulin, S.A. Zapunidy, M.S. Pshenichnikov, P.H.M.v. Loosdrecht, D.Yu. Paraschuk, Phys. Chem. Chem. Phys. 11 (2009) 7324.
[12] A.A. Bakulin et al., Synth. Met. 147 (2004) 221.
[13] A.A. Bakulin, D.S. Martyanov, D.Yu. Paraschuk, M.S. Pshenichnikov, P.H.M. van Loosdrecht, J. Phys. Chem. B 112 (2008) 13730.
[14] X. Wei, Z.V. Vardeny, N.S. Sariciftci, A.J. Heeger, Phys. Rev. B 53 (1996) 2187.
[15] J.G. Müller et al., Phys. Rev. B 72 (2005) 195208.
[16] S. Westenhoff et al., J. Am. Chem. Soc. 130 (2008) 13653.
[17] S. Singh, T. Drori, Z.V. Vardeny, Phys. Rev. B 77 (2008).
[18] S. Yeremenko, A. Baltuska, F. de Haan, M.S. Pshenichnikov, D.A. Wiersma, Opt. Lett. 27 (2002) 1171.
[19] V.V. Bruevich, T.S. Makhmutov, S.G. Elizarov, E.M. Nechvolodova, D.Yu. Paraschuk, J. Chem. Phys. 127 (2007) 104905.
[20] N.-K. Persson, X. Wang, O. Inganäs, Appl. Phys. Lett. 91 (2007) 083503.
[21] J. Gilot, I. Barbu, M.M. Wienk, R.A.J. Janssen, Appl. Phys. Lett. 91 (2007) 113520.
[22] S.E. Shaheen, C.J. Brabec, N.S. Sariciftci, F. Padinger, T. Fromherz, J.C. Hummelen, Appl. Phys. Lett. 78 (2001) 841.
[23] R.A.J. Janssen, M.P.T. Christiaans, C. Hare, N. Martin, N.S. Sariciftci, A.J. Heeger, F. Wudl, J. Chem. Phys. 103 (1995) 8840.
[24] S.P. McGlynn, Chem. Rev. 58 (1958) 1113.
[25] D.Yu. Paraschuk, S.G. Elizarov, A.N. Khodarev, A.N. Shchegolikhin, S.A. Arnautov, E.M. Nechvolodova, JETP Lett. 81 (2005) 583.
[26] J. Holt, S. Singh, T. Drori, Y. Zheng, Z.V. Vardeny, Phys. Rev. B 79 (2009).
[27] S.G. Elizarov, A.E. Ozimova, D.Yu. Paraschuk, S.A. Arnautov, E.M. Nechvolodova, Proc. SPIE 6257 (2006) 293.
[28] J.J.M. Halls, K. Pichler, R.H. Friend, S.C. Moratti, A.B. Holmes, Appl. Phys. Lett. 68 (1996) 3120.
[29] S.A. Zapunidi, Y.V. Krylova, D.Yu. Paraschuk, Phys. Rev. B 79 (2009).
[30] V.I. Arkhipov, P. Heremans, H. Bassler, Appl. Phys. Lett. 82 (2003) 4605.